A THERMODYNAMIC ANALYSIS OF THE PROCESS OF HYDROGEN PRODUCTION BY NATURAL GAS DECOMPOSITION IN THE LOW-TEMPERATURE THERMAL PLASMA REACTOR

Nada Milutinović*,1, Aleksandar Erić[1], Dejan Cvetinović[1],
Nikola Živković[1], and Jovana Anđelković[1]

[1] Vinca Institute of Nuclear Sciences, National Institute of
the Republic of Serbia, Laboratory for Thermal Engineering and Energy,
Mike Petrovića Alasa 12-14, 11351 Vinča, Belgrade, Serbia [1]

Abstract: Hydrogen produced via the thermal decomposition of natural gas, also known as 'turquoise' hydrogen, is the subject of this study. It is expected that 'turquoise' hydrogen will play a significant role in the coming energy transition, reducing emissions from fossil fuels in the short term until renewable energy sources are capable of producing enough energy or hydrogen transport becomes feasible on a large scale. The main advantage of the thermal decomposition of natural gas is the possibility of obtaining a high yield of hydrogen without the emission of carbon monoxide or carbon dioxide since the main products of the process are carbon in a solid state and hydrogen. The use of plasma in the process elevates the temperature of the process and increases methane decomposition without the use of catalysts. This paper presents an analysis of the process using a thermodynamic equilibrium model based on the minimum of the Gibbs function in the temperature range of 500-2000 K. As a result of the study, the equilibrium composition of the system in the observed temperature range is presented. Also, attention is given to undesirable components in the system such as carbon dioxide, hydrocyanic acid, and nitrogen compounds like ammonia and nitrogen monoxide. From the point of energy analysis, the useful energy of the system per kilogram of fuel and the efficiency of the process is presented. The results of the numerical analysis show that the efficiency of the process increases with increasing temperature and reaches its maximum at a temperature of 1200 K when an energy efficiency of about 50% is achieved.

Keywords: hydrogen, natural gas, plasma, pyrolysis

1. INTRODUCTION

With the introduction of the Renewable Energy Directive (2009/28/EC) in 2009, the share of renewable sources has kept growing yearly, reaching 22% in 2020. The Renewable Energy Directive was revised many times to make a path for reaching climate neutrality by 2050. The previous goal for the share of renewables in the EU's energy consumption by 2030 was 32%. In July 2021, the goal increased to 40%, while recently, in September 2022 it increased again to 45% [1]. Hydrogen has been identified as one of the key alternatives for achieving the net zero greenhouse gasses (GHGs) emissions commitments that governments have announced in past years. According to the work of Ajanović et al. [2] hydrogen can be classified as 'grey', 'blue', 'turquoise', 'green', and 'purple', which is presented in Fig. 1. In 2021, hydrogen demand reached 94 million tonnes (Mt) which resulted in GHG emissions of 900 Mt CO_2 [3]. Hydrogen was used in refineries to remove impurities such as sulfur (40 Mt), in the industry sector to produce ammonia (34 Mt) and methanol (15 Mt), in the steel industry (5 Mt), in transport for heavyweight road and rail vehicles (30 kt), while hydrogen demand in the building and power sector accounted for a negligible. The majority of hydrogen demand in 2021 was met by 'grey' hydrogen where 62% was produced from natural gas, 18% of hydrogen was produced from naphtha reforming at refineries, and 19% from coal, therefore there were no environmental benefits from lower GHGs emissions. At the same time, 'blue' hydrogen production was less than 1 Mt [3]. Nevertheless, 'blue' and 'turquoise' hydrogen will play a significant role in the following energy transition, in particular, to reduce the emissions from fossil fuels in the short term until enough energy can be produced from renewable sources or until hydrogen transport would be possible on a big scale.

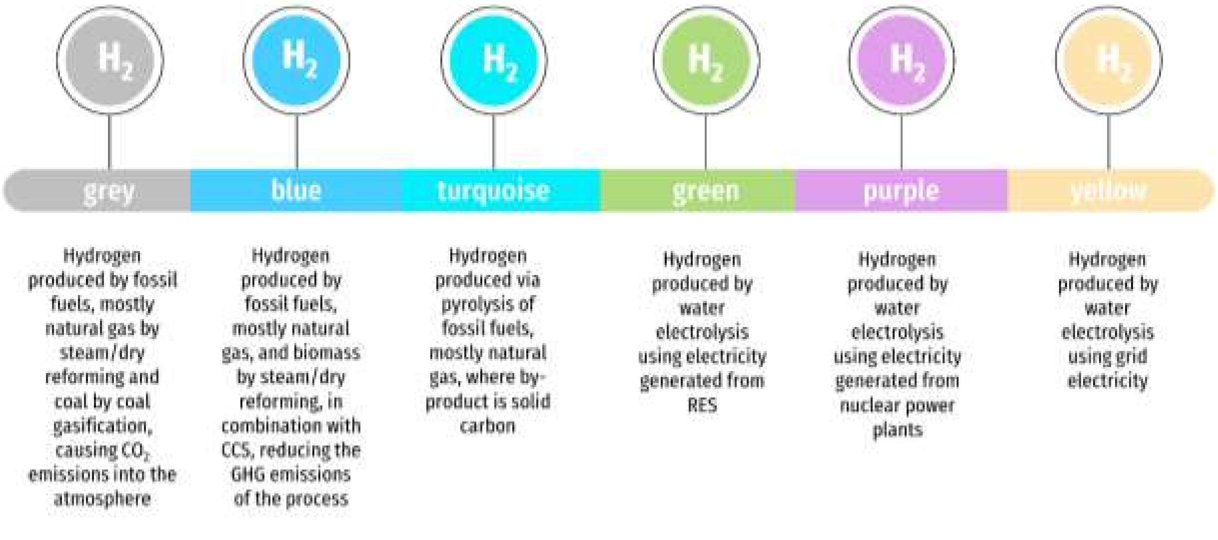

Fig. 1 The colors of hydrogen, adapted from [2]

The merits and demerits of the most popular hydrogen-producing technologies such as natural gas reforming, water electrolysis, and photobiological and thermochemical methods are presented in the work of Bespalko et al. [4]. Hydrogen can be produced from natural gas by various processes: steam methane reforming (SMR), dry methane reforming (DMR), partial oxidation (POx), and thermal decomposition (TD). SMR uses methane from natural gas which reacts with steam under pressure 0.3-2.5 MPa in the presence of a usually nickel-based or alumina catalyst and transforms it into syngas, which is a mixture of hydrogen, carbon monoxide, and a small number of other components [5], [6]. The process is conducted at temperatures higher than 800°C which are often achieved by the combustion of some methane feed gas [7], [8]. In the case of DMR, methane reacts with carbon dioxide to produce syngas with an H_2/CO molar ratio close to 1. Both previous processes are endothermic, meaning they require high energy demand. On the other hand, POx is an exothermic reaction with the advantage of reducing energy demand for the reforming process. Produced syngas from the previously mentioned technologies is then shifted into a hydrogen-rich mixture in a reactor where high-purity hydrogen can be obtained by water-gas shift (WGS) reaction where produced carbon monoxide reacts with steam which results in more hydrogen. WGS reaction on the other hand may lead to excessive carbon dioxide generation in hydrogen-rich gas, as reported in the work of Shagdar et al. [9]. Pressure swing adsorption (PSA) is used as a final stage to remove mainly carbon dioxide, but also water, methane, and carbon monoxide from the hydrogen-rich gas [10] and obtain high-purity hydrogen of 99% [6]. Thermal decomposition of methane sometimes referred to as pyrolysis [11] or methane cracking [12] is a process of decomposing methane into carbon and hydrogen without producing carbon dioxide or monoxide [13] which makes it a very attractive technology since does not need carbon capture, utilization, and storage system (CCUS). The decomposition of methane starts at 500-600°C, but to obtain a high yield of hydrogen, significantly higher temperatures should be used, especially if the process is conducted without the catalyst. It is worth mentioning that during the decomposition process, the carbon produced as a by-product may play a catalytic role and increase the conversion of methane and hydrogen yield [14].

Steam methane reforming (SMR)	$CH_4 + H_2O \rightarrow CO + 3H_2$	$\Delta H^0_{298} = 206$ kJ/mol	[5]
Dry methane reforming (DMR)	$CH_4 + CO_2 \rightarrow 2H_2 + 2CO$	$\Delta H^0_{298} = 247$ kJ/mol	[5]
Partial oxidation (POx)	$CH_4 + 0.5O_2 \rightarrow CO + 2H_2$	$\Delta H^0_{298} = -36$ kJ/mol	[8]
Water-gas shift reaction (WGS)	$CO + H_2O \rightarrow CO_2 + H_2$	$\Delta H^0_{298} = -41.2$ kJ/mol	[8]
Thermal decomposition (TD)	$CH_4 \rightarrow C(s) + 2H_2$	$\Delta H^0_{298} = 74.52$ kJ/mol	[15]

Hrabovsky et al. [5] have stressed the limitations of mentioned technologies which are related to the necessity of catalyst usage to obtain high conversion levels of methane. Park et al. [8] and Iulianelli et al. [16] also pointed out that studies related to these processes pay high attention to the catalysts used in the process and its activity and stability, the effect of the type and amount of active metal on catalyst performance, identification of causes of deactivation like sintering of metallic species and coke deposition. Fan et al. [17] reported that it is difficult for the catalysts to exhibit high activity and long-term stability at the same time, so most solid catalysts have a lifetime of less than 10 h. Finding the appropriate candidate catalysts for the SRM process is a big technical challenge since the use of catalysts highly affects the performance of the process. Amongst the most investigated catalysts are materials including Ni, Fe, Co, Al, Ru, Rh, Pd, Ir, and Pt [18]. Choi et al. [7] also added that the use of noble metals as catalysts is expensive and prone to contamination with species such as sulfur, and suggested using steam plasma reforming without a catalyst.

Using plasma in the methane conversion processes possesses various benefits such as high quality of the produced syngas, easy control of its composition, compatibility for a wide range of hydrocarbons (natural gas, heavy oils, and biofuels), also compactness and fast response time since plasma is operated by electricity, and no need for catalysts, therefore, no risk of catalyst sensitivity and deterioration [5], [7], [19]. As a result of high temperatures and high ionization which correspond to the plasma conditions, thermodynamically favorable chemical reactions can be accelerated without using a catalyst, as well as endothermic reforming processes can be provided with energy [20]. Different types of non-thermal and thermal plasmas have already been used for the conversion of methane into hydrogen, amongst non-thermal plasmas are dielectric-barrier discharges (DBD) [21], [22] and gliding arc discharge [23], [24], while amongst thermal plasmas are alternating current (AC) [25], radio frequency (RF) [26], microwave plasmas (MW) [7], [27]–[29], and also hybrid modifications are available such as direct current (DC)-spark discharge plasma [30], AC-gliding arc discharge [31], DC-RF [32], etc.

Hrabovsky et al. [5] studied dry and steam methane reforming in the thermal plasma and carried out calculations on the equilibrium composition of reaction products and energy balances. The observed temperature range was 400-6000 K, the pressure was 0.1 MPa, and substances that were taken into account were: C_2, C_3, CO, CO_2, C_3O_2, CH, CH_2, CH_3, CH_4, HCO, H_2CO, C_2H, C_2H_2, C_2H_4, O_2, O_3, H_2, OH, HO_2, H_2O, and H_2O_2. The equilibrium composition of syngas for steam methane reforming presented a significantly higher yield of hydrogen and hydrogen in atom form compared to dry steam reforming where carbon monoxide yield was higher compared to the hydrogen yield. The authors also conducted experimental research and reported that the minimum energy needed for the production of 1 kg of hydrogen was 79 MJ for steam reforming and 116 MJ for dry reforming and it corresponds to the energy spent for the process in the reactor volume, not the total energy consumed which includes torch efficiency and power loss in the reactor. Czylkowski et al. [28] presented experimental results of hydrogen production by atmospheric microwave plasma combined with steam reforming of methane. They observed the hydrogen production rate (how many grams of hydrogen are produced per 1 h), the energy yield of hydrogen production (the ratio of hydrogen production rate to the absorbed microwave power), the methane conversion degree, and the volume concentration of hydrogen in the outlet gas. The results stated the absorbed microwave power was in the range of 3.5 to 4.5 kW, and the hydrogen production rate, the methane conversion degree, and the hydrogen concentration increased, while the energy yield decreased with increasing absorbed microwave power. The best-achieved results of hydrogen production rate and energy yield were 192 gH_2/h and 42.9 gH_2/kWh, respectively. Abanades et al. [33] reported that in the case of catalytic cracking temperatures are below 1000°C, but the problem is the deactivation of catalyst by coke formation.

Further research on methane cracking is necessary since the main requirement for the development of a reliable hydrogen production technology that can be implemented on a large scale is to be able to operate in continuous mode which has not yet been achieved. This paper presents the results of a numerical investigation of the thermal plasma decomposition process of natural gas to obtain a high yield of hydrogen. The used equilibrium model is based on the minimum of the Gibbs function and has been explained in our previous work [34]–[36] on cases of agricultural biomass and hazardous waste in steam or air plasma gasification. The study aims to demonstrate the effectiveness of the suggested operating conditions on the efficiency of the process. The parameters of interest are the equilibrium composition of the system at the analyzed temperature range with special attention to the undesired components such as carbon dioxide, hydrocyanic acid, and nitrogen compounds, as well as a ratio of useful and the input power of the system.

2. MATERIALS AND METHODS

2.1. Thermodynamic equilibrium model

By modifying the Clausius inequality for irreversible processes under the assumption that the system is at constant pressure, the condition of the spontaneity of the process is reached in the following form

$$dS_{p,H} \geq \tag{1}$$

$$dH_{p,S} \leq \tag{2}$$

Based on these equations, a process in a system at constant pressure and temperature is spontaneous if the total entropy change (system and environment) is greater than zero, and the enthalpy change is less than zero.

The enthalpy possessed by a thermodynamic system can be used partially, which depends on the state of the environment, so it consists of a usable and an unusable part. The maximum possible energy that can be obtained at constant pressure from a system is essentially the maximum non-expansion work or Gibbs free energy, which can be determined as

$$G = \quad - \tag{3}$$

In the case of a system consisting of two or more components, the total value of the Gibbs function will be equal to the sum of the Gibbs functions of all components

$$G = \sum_{j} \tag{4}$$

When it comes to a system consisting of several components, the concept of chemical reactivity of each component is introduced, as a special state quantity. This parameter represents the maximum energy, that is, the ability of each component to influence the change in the composition of the system. Looking back at the definition of Gibbs energy, as the maximum available energy of the system, it is concluded that chemical reactivity is nothing but a partial molar Gibbs function. Therefore, Eq. (4) can be written in the following form

$$G = \sum_{j} \tag{5}$$

where is

$$\mu_j = \quad + \quad \frac{i}{p_0} \tag{6}$$

The pressure ratio in Eq. (6) can be defined as the activity of the corresponding component and based on that, the following expression is obtained

$$\mu_j = \quad + \tag{7}$$

By differentiating Eq. (7) and combining the Gibbs-Duem equation

$$\sum_{j} \tag{8}$$

the expression for the change in the Gibbs function at constant pressure and temperature is obtained

$$dG = \sum_{j} \tag{9}$$

According to the Second Law of Thermodynamics, the condition for the spontaneity of a process is an increase in the total entropy of the system and environment, therefore from Eq. (2), it can be seen that the condition for the spontaneity of a process that takes place in a system at constant pressure and temperature is that the enthalpy change is negative. As it was mentioned that the Gibbs function, i.e. the Gibbs free energy is nothing but the "usable part of the enthalpy", the condition for the spontaneity of a process that takes place in a system at constant pressure at a certain temperature is the reduction of the Gibbs free energy

$$dG_{T,p} < \tag{10}$$

This reduction takes place until the moment when the change of the function becomes equal to zero, which means that at that moment the system has reached the minimum of the Gibbs function [37]

$$dG = \qquad (11)$$

If we now look at the system of *j*-components in which the reactions take place, the total molar Gibbs function of the reaction is equal to the difference between the molar Gibbs functions of the final components and the starting components

$$\Delta \quad = \sum_{p_i} \qquad \sum \qquad (12)$$

Using Donder's relation and the fact that the partial derivative of the Gibbs function by the volume of the reaction is equal to the partial molar Gibbs function, Eq. (12) can be written in the following form

$$\Delta \quad = \sum_{p_i} \qquad \sum \qquad (13)$$

According to Dalton's law, the pressure in a system consisting of *j* components is equal to the sum of the partial pressures of all components, which means that the chemical potential of the component in the mixture must be expressed depending on its partial pressure. Applying the conditions of chemical equilibrium, the following can be written

$$0 = \cdot + \cdot \quad {}_{p_0} - \cdot - \cdot \quad {}_{p_0} \qquad (14)$$

By grouping the terms related to the chemical potential of products and reactants at standard conditions and introducing activities, a simpler expression is obtained

$$0 = \Delta \quad + \quad \frac{{}^{\nu_P}_{p}}{a_R^{\nu_R}} \qquad (15)$$

or

$$\Delta \quad = - \quad \prod \qquad (16)$$

where Δ represents the difference of standard molar Gibbs energies of products and reactants.

The equilibrium composition of the system consisting of *j* components is uniquely determined by Eq. (16) and the condition that the partial molar Gibbs function has the lowest possible value [38].

The enthalpy of a system that is in an equilibrium state is the quantity of the state whose value at a certain temperature consists of the physical enthalpy and the enthalpy of formation of the components

$$H = \quad + \Delta \qquad (17)$$

The absolute value of physical enthalpy is not easy to determine, but it is not necessary to know its absolute value, only the value of its change between the initial and final state of the system. This defines the amount of heat exchanged between the system and the environment, which is the most important when it comes to thermochemistry. In general, the value of the physical enthalpy of the system in the final state when changing from the initial state is

$$H^0 = \quad + \int_{ref}^{T} \tag{18}$$

By observing a system consisting of *n* components, the enthalpy value of the jth component can be written in the following form

$$H_j \; T - \quad = \quad - \quad + \Delta \tag{19}$$

For the entire system consisting of *j* components, the enthalpy difference between the reference and specified temperature is defined as follows

$$H_s \; T - \quad = \sum \quad \sum \tag{20}$$

By introducing a shift in the form of the Gibbs-Helmholtz equation, Eq. (20) becomes

$$H_s \; T - \quad = \sum \quad \sum \tag{21}$$

In thermochemistry, it is customary to calculate the values of all enthalpies concerning the reference state, so it can be assumed that the enthalpy value in the reference state is equal to zero, for the sake of understanding, it is especially acceptable if the reference temperature is equal to absolute zero. In that case, the total enthalpy of the system has the apparent form of an absolute value

$$H_s \; T = \sum \quad \sum \tag{22}$$

2.2. Mass and energy balance

This paper discusses the process of thermal decomposition or pyrolysis of methane, the main constituent of natural gas, in a low-temperature plasma reactor to obtain a high yield of hydrogen. The composition and characteristics of the natural gas used in the model are given in Tab. 1.

Table 1. Natural gas composition and characteristics at the reactor inlet

Gas components				Lower heating value	Higher heating value	Density
CH_4	C_2H_6	N_2	CO_2	H_d	H_g	ρ_g
%vol				kJ/m^3	kWh/m^3	kg/m^3
95.96	2.16	0.72	0.28	34,798.00	11.31	0.71

It was assumed that the fuel (natural gas) enters the plasma reactor at a temperature of 25°C (298.15K), passes through an electric arc, and at the outlet the components of the system are obtained which are in thermodynamic equilibrium at a certain (desired) temperature. Passing through the plasma reactor, the fuel receives the energy of the electric arc, as a result of which the covalent bonds in the hydrocarbon molecules (CH_4 and C_2H_6) are broken and carbon is formed in the solid phase (graphite) and hydrogen (H_2). Even though the dissociation of hydrogen occurs at higher temperatures, above 2000 K, it is not of interest in this study, because when cooling the system, the dissociated hydrogen atoms very quickly rebuild into a stable hydrogen molecule. Carbon in a solid state, which is a by-product of the process, is most often in the form of graphite, i.e. soot, so in this research, it will be considered an undesirable side effect. Otherwise, high temperatures and the presence of a large amount of carbon in the reactor are suitable for the process of creating other compounds containing carbon, such as calcium carbide (CaC_2), silicon carbide (SiC), and many others.

Based on the above assumptions, the energy balance of the thermodynamic system can be set in the following form

$$\dot{r} \qquad \cdot \tag{23}$$

giving the equation for the required power of a plasma reactor in the form of

$$P_p\ T = \cdot \qquad - \tag{24}$$

The input power is equal to the sum of the power supplied by the fuel and the power of the plasma. The power supplied by the fuel is then defined as the product of the fuel mass flow and the lower heating value (LHV) at the reference temperature

$$P_i\ T = \quad + \qquad = \cdot \qquad - \tag{25}$$

The useful power or the power of the obtained hydrogen can be defined as the product of the flow rate and the lower heating value of hydrogen

$$P_{H_2}\ T = \cdot \tag{26}$$

If the efficiency of the considered process is equal to the ratio of useful and input power

$$\eta\ T = \frac{P\ \ T}{P_i\ T} = \frac{\cdot}{\dot{r}} \tag{27}$$

3. RESULTS AND DISCUSSION

Fig. 2-4 show the equilibrium composition of the system depending on the temperature, determined by the presented methodology of pyrolysis of natural gas in a low-temperature plasma reactor.

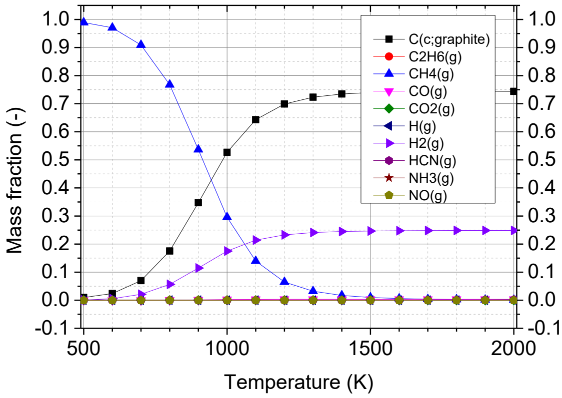

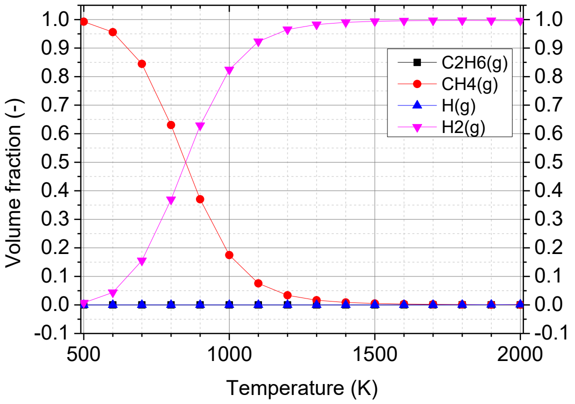

Fig. 2 Mass fractions of system components

Fig. 3 Volume fraction of system components

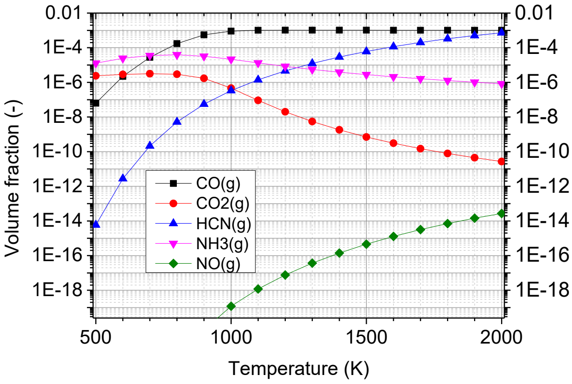

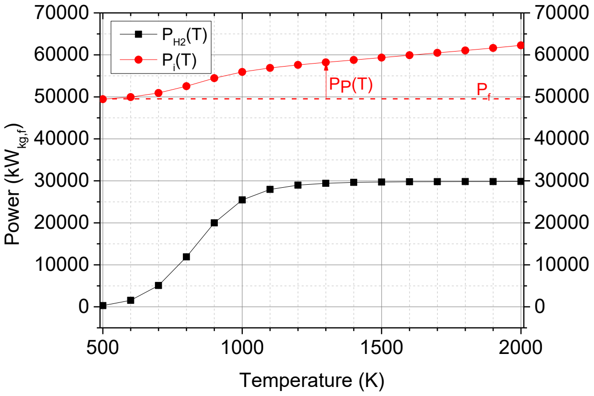

Fig. 4 Volume fraction of undesirable system components

Fig. 5 Useful power and input power

Fig 1-2 clearly show that the share of combustible components, primary methane, decreases with increasing temperature, while the share of graphite and hydrogen in molecular form increases in proportion to its decrease. This process is practically completed at a temperature of 1500 K. Undesirable components of the system are shown in Fig. 3, where it is noticeable that with increasing temperature the proportion of hydrocyanic acid and nitrogen monoxide increases, while the proportion of ammonia and carbon dioxide decreases. The share of carbon monoxide increases intensively up to a temperature of 1000 K, after which its growth stops and the value does not change with a further increase in temperature. Bearing in mind that the proportions of nitrogen monoxide and hydrocyanic acid increase more intensively than the proportions of ammonia and carbon dioxide decrease with increasing temperature, as well as the fact of the harmfulness of the first two undesirable compounds, it can be concluded that from this point of view a lower temperature is more suitable.

The energy analysis, shown in Fig. 4, shows that the useful energy of the system per kilogram of fuel increases with the increase in process temperature and reaches a maximum value of around 1500 K, after which it remains constant with a further increase in temperature. This is expected considering that the maximum fuel conversion occurred in the process, i.e. the complete pyrolysis of natural gas occurred and the maximum possible concentration of hydrogen was achieved. The input power per kilogram of fuel consists of the power input by the fuel (natural gas) and the plasma reactor power. The power of the fuel is a constant value and is defined by the mass flow of the fuel and its thermal power, while the power of the plasma reactor increases with the increase in temperature. Unlike the output power, this power increases as expected, although the pyrolysis process ends at 1500 K. Therefore, it is obvious that further increasing the temperature of the process above 1500 K does not make any sense, the additional energy would be spent on further increasing the physical enthalpy of the products, the formation of undesirable compounds as well as on the dissociation of hydrogen. None of the mentioned processes are desirable during the pyrolysis of natural gas. Increasing the physical enthalpy does not make sense, considering that after reaching the equilibrium concentration of the system at the desired temperature, it is necessary to cool it very quickly, so-called quenching to prevent the reversibility of the process, as well as the formation of undesirable compounds that would eventually be formed in the process of slow cooling. Considering that the heat removed in the process of quenching the system represents a pure loss of the process, it is clear why a further increase in temperature is undesirable.

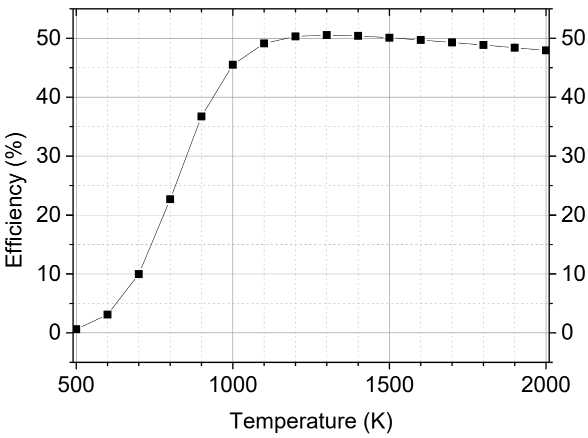

Fig. 5 The efficiency of the process

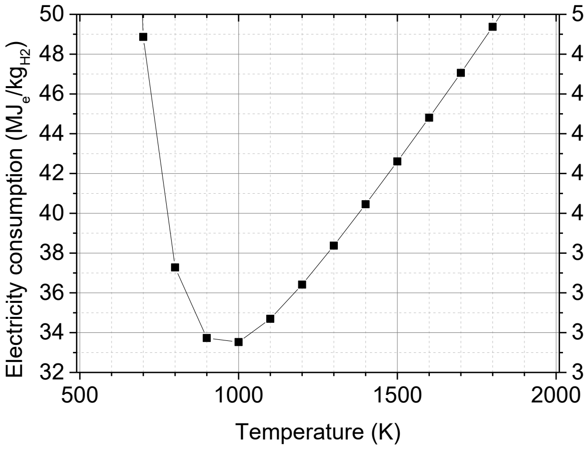

Fig. 6 Electricity consumption

The energy at the inlet to the system is equal to the sum of useful energy and energy losses. The energy losses consist of the energy contained in the graphite by-product, the energy removed from the system by quenching, and other energy losses which are an order of magnitude smaller than the mentioned two. The efficiency of the process is shown in Fig. 5.

From Fig. 5, it can be seen that the efficiency of the process increases with increasing temperature and reaches a maximum at a temperature of around 1200 K and is around 50%. However, as previously analyzed, at this temperature the process of pyrolysis of natural gas is not completely completed, i.e. the proportion of hydrogen has not reached its maximum. In the temperature range of

1200-1500K, the increase in hydrogen content is about 1.3% compared to the total value, and the increase in plasma reactor power is about 17%, which means that plasmatron energy is mainly spent on increasing the physical enthalpy of the system. Bearing in mind that the increase in the physical enthalpy of the system is a pure loss, as well as that the increase in the proportion of hydrogen is negligible, it follows that the optimal temperature for the natural gas pyrolysis process is 1200 K considered from the point of view of energy analysis.

Fig. 6 shows the consumption of electricity for hydrogen production, assuming that the degree of conversion to plasma energy is 100%. It can be seen from the picture that for the production of one kilogram of hydrogen at a temperature of 1200 K, about 36.5 MJ is needed.

4. CONCLUSION

The paper discusses the process of pyrolysis of natural gas to obtain hydrogen in a low-temperature plasma reactor. The hydrogen yield was determined based on the calculation of the equilibrium composition of the system using the Gibbs free energy minimization methodology. The applied methodology obtained the temperature dependence of the equilibrium composition of the system. The results of the one-dimensional numerical analysis show that the efficiency of the process increases with increasing temperature and reaches its maximum at a temperature of 1200K when an energy efficiency of about 60% is achieved. The resulting system must be cooled (quenched) very quickly to prevent reversibility and the formation of undesirable compounds. During the analysis of the process, it was assumed that the only useful product is hydrogen, while carbon in the form of graphite was considered a by-product. It is certainly possible to use graphite in some other form, but this may be the subject of new research in this area. In the process of pyrolysis of natural gas, undesirable and harmful compounds are formed, primarily carbon monoxide, ammonia, hydrocyanic acid, and nitrogen monoxide. The analysis of the obtained results showed that from the point of view of ecology, a lower process temperature is more favorable. The developed model of the natural gas pyrolysis process in a low-temperature plasma reactor opens up possibilities for further research aimed at the utilization of graphite by-products as well as the utilization of waste heat from the quenching process of the system. In addition, further analysis can be directed to the process of gasification of natural gas in a low-temperature plasma reactor using water as a working medium.

ACKNOWLEDGEMENT

The research was funded by the Ministry of Education, Science and Technological Development of the Republic of Serbia, Grant no. 451-03-09/2021-14/200017 («Vinča» Institute of Nuclear Sciences, National Institute of the Republic of Serbia, University of Belgrade).

REFERENCES

[1] **, “The Renewable Energy Directive .” https://energy.ec.europa.eu/topics/renewable-energy/renewable-energy-directive-targets-and-rules/renewable-energy-directive_en (accessed Oct. 27, 2022).

[2] A. Ajanovic, M. Sayer, and R. Haas, “The economics and the environmental benignity of different colors of hydrogen,” *Int J Hydrogen Energy*, vol. 47, no. 57, pp. 24136–24154, 2022, doi: 10.1016/j.ijhydene.2022.02.094.

[3] International Energy Agency (IEA), “Global Hydrogen Review 2022,” 2022. [Online]. Available: www.iea.org/t&c/

[4] S. Bespalko and J. Mizeraczyk, “Overview of the Hydrogen Production by Plasma-Driven Solution Electrolysis,” *Energies (Basel)*, vol. 15, no. 20, p. 7508, 2022, doi: 10.3390/en15207508.

[5] M. Hrabovsky *et al.*, “Steam Plasma Methane Reforming for Hydrogen Production,” *Plasma Chemistry and Plasma Processing*, vol. 38, no. 4, pp. 743–758, 2018, doi: 10.1007/s11090-018-9891-5.

[6] L. Barelli, G. Bidini, F. Gallorini, and S. Servili, “Hydrogen production through sorption-enhanced steam methane reforming and membrane technology: A review,” *Energy*, vol. 33, no. 4, pp. 554–570, 2008, doi: 10.1016/j.energy.2007.10.018.

[7] D. H. Choi, S. M. Chun, S. H. Ma, and Y. C. Hong, “Production of hydrogen-rich syngas from methane reforming by steam microwave plasma,” *Journal of Industrial and Engineering Chemistry*, vol. 34, pp. 286–291, 2016, doi: 10.1016/j.jiec.2015.11.019.

[8] H.-G. Park, S.-Y. Han, K.-W. Jun, Y. Woo, M.-J. Park, and S. K. Kim, “Bench-Scale Steam Reforming of Methane for Hydrogen Production,” *Catalysts*, vol. 9, no. 7, p. 615, 2019, doi: 10.3390/catal9070615.

[9] E. Shagdar, B. G. Lougou, Y. Shuai, E. Ganbold, O. P. Chinonso, and H. Tan, “Process analysis of solar steam reforming of methane for producing low-carbon hydrogen,” *RSC Adv*, vol. 10, no. 21, pp. 12582–12597, 2020, doi: 10.1039/C9RA09835F.

[10] K. S. Go, S. R. Son, S. D. Kim, K. S. Kang, and C. S. Park, “Hydrogen production from two-step steam methane reforming in a fluidized bed reactor,” *Int J Hydrogen Energy*, vol. 34, no. 3, pp. 1301–1309, 2009, doi: 10.1016/j.ijhydene.2008.11.062.

[11] S. Timmerberg, M. Kaltschmitt, and M. Finkbeiner, “Hydrogen and hydrogen-derived fuels through methane decomposition of natural gas – GHG emissions and costs,” *Energy Conversion and Management: X*, vol. 7, p. 100043, 2020, doi: 10.1016/j.ecmx.2020.100043.

[12] L. Weger, A. Abánades, and T. Butler, “Methane cracking as a bridge technology to the hydrogen economy,” *Int J Hydrogen Energy*, vol. 42, no. 1, pp. 720–731, 2017, doi: 10.1016/j.ijhydene.2016.11.029.

[13] H. F. Abbas and W. M. A. Wan Daud, “Hydrogen production by methane decomposition: A review,” *Int J Hydrogen Energy*, vol. 35, no. 3, pp. 1160–1190, 2010, doi: 10.1016/j.ijhydene.2009.11.036.

[14] M. Yousefi and S. Donne, “Technical challenges for developing thermal methane cracking in small or medium scales to produce pure hydrogen - A review,” *Int J Hydrogen Energy*, vol. 47, no. 2, pp. 699–727, 2022, doi: 10.1016/j.ijhydene.2021.10.100.

[15] J. X. Qian, T. W. Chen, L. R. Enakonda, D. bin Liu, J.-M. Basset, and L. Zhou, “Methane decomposition to pure hydrogen and carbon nano materials: State-of-the-art and future perspectives,” *Int J Hydrogen Energy*, vol. 45, no. 32, pp. 15721–15743, 2020, doi: 10.1016/j.ijhydene.2020.04.100.

[16] A. Iulianelli, S. Liguori, J. Wilcox, and A. Basile, “Advances on methane steam reforming to produce hydrogen through membrane reactors technology: A review,” *Catalysis Reviews*, vol. 58, no. 1, pp. 1–35, 2016, doi: 10.1080/01614940.2015.1099882.

[17] Z. Fan, W. Weng, J. Zhou, D. Gu, and W. Xiao, “Catalytic decomposition of methane to produce hydrogen: A review,” *Journal of Energy Chemistry*, vol. 58, pp. 415–430, 2021, doi: 10.1016/j.jechem.2020.10.049.

[18] L. Chen, Z. Qi, S. Zhang, J. Su, and G. A. Somorjai, “Catalytic Hydrogen Production from Methane: A Review on Recent Progress and Prospect,” *Catalysts*, vol. 10, no. 8, p. 858, 2020, doi: 10.3390/catal10080858.

[19] P. Stefanović, P. Pavlović, Ž. Kostić, and D. Cvetinović, “Plazma proces proizvodnje čađi i vodonika iz metana,” in *GAS ’97*, 1997, pp. 340–348.

[20] L. Bromberg, D. R. Cohn, A. Rabinovich, and N. Alexeev, “Plasma catalytic reforming of methane.”

[21] F. Saleem, J. Harris, K. Zhang, and A. Harvey, “Non-thermal plasma as a promising route for the removal of tar from the product gas of biomass gasification – A critical review,” *Chemical Engineering Journal*, vol. 382, no. June 2019, p. 122761, 2020, doi: 10.1016/j.cej.2019.122761.

[22] A. H. Khoja *et al.*, “Hydrogen Production from Methane Cracking in Dielectric Barrier Discharge Catalytic Plasma Reactor Using a Nanocatalyst,” *Energies (Basel)*, vol. 13, no. 22, p. 5921, 2020, doi: 10.3390/en13225921.

[23] C. S. Kalra, A. F. Gutsol, and A. A. Fridman, “Gliding arc discharges as a source of intermediate plasma for methane partial oxidation,” *IEEE Transactions on Plasma Science*, vol. 33, no. 1, pp. 32–41, Feb. 2005, doi: 10.1109/TPS.2004.842321.

[24] X. Guofeng and D. Xinwei, “Optimization geometries of a vortex gliding-arc reactor for partial oxidation of methane,” *Energy*, vol. 47, no. 1, pp. 333–339, Nov. 2012, doi: 10.1016/j.energy.2012.09.032.

[25] M. Gautier, V. Rohani, and L. Fulcheri, “Direct decarbonization of methane by thermal plasma for the production of hydrogen and high value-added carbon black,” *Int J Hydrogen Energy*, vol. 42, no. 47, pp. 28140–28156, 2017, doi: 10.1016/j.ijhydene.2017.09.021.

[26] A. E. E. Putra, S. Nomura, S. Mukasa, and H. Toyota, “Hydrogen production by radio frequency plasma stimulation in methane hydrate at atmospheric pressure,” *Int J Hydrogen Energy*, vol. 37, no. 21, pp. 16000–16005, 2012, doi: 10.1016/j.ijhydene.2012.07.099.

[27] O. Akande and B. Lee, “Plasma steam methane reforming (PSMR) using a microwave torch for commercial-scale distributed hydrogen production,” *Int J Hydrogen Energy*, vol. 47, no. 5, pp. 2874–2884, 2022, doi: 10.1016/j.ijhydene.2021.10.258.

[28] D. Czylkowski, B. Hrycak, M. Jasiński, M. Dors, and J. Mizeraczyk, “Microwave plasma-based method of hydrogen production via combined steam reforming of methane,” *Energy*, vol. 113, pp. 653–661, 2016, doi: 10.1016/j.energy.2016.07.088.

[29] Q. Wang, J. Wang, T. Zhu, X. Zhu, and B. Sun, “Characteristics of methane wet reforming driven by microwave plasma in liquid phase for hydrogen production,” *Int J Hydrogen Energy*, vol. 46, no. 69, pp. 34105–34115, 2021, doi: 10.1016/j.ijhydene.2021.08.006.

[30] M. M. Moshrefi, F. Rashidi, H. R. Bozorgzadeh, and S. M. Zekordi, “Methane Conversion to Hydrogen and Carbon Black by DC-Spark Discharge,” *Plasma Chemistry and Plasma Processing*, vol. 32, no. 6, pp. 1157–1168, 2012, doi: 10.1007/s11090-012-9408-6.

[31] X. Tu and J. C. Whitehead, “Plasma dry reforming of methane in an atmospheric pressure AC gliding arc discharge: Co-generation of syngas and carbon

nanomaterials," *Int J Hydrogen Energy*, vol. 39, no. 18, pp. 9658–9669, 2014, doi: 10.1016/j.ijhydene.2014.04.073.

[32] Keun Su Kim, Jun Ho Seo, Jun Seok Nam, Won Tae Ju, and Sang Hee Hong, "Production of hydrogen and carbon black by methane decomposition using DC-RF hybrid thermal plasmas," *IEEE Transactions on Plasma Science*, vol. 33, no. 2, pp. 813–823, 2005, doi: 10.1109/TPS.2005.844526.

[33] A. Abánades, C. Rubbia, and D. Salmieri, "Thermal cracking of methane into Hydrogen for a CO2-free utilization of natural gas," *Int J Hydrogen Energy*, vol. 38, no. 20, pp. 8491–8496, 2013, doi: 10.1016/j.ijhydene.2012.08.138.

[34] D. Cvetinović, A. Erić, P. Škobalj, N. Milutinović, and V. Bakić, "Thermodynamic Modeling as a Tool for Design and Optimisation of Thermal Plasma Reactor for PCBs Decomposition," in *5th Conference on Sustainable Development of Energy, Water and Environment Systems*, 2022, p. 224.

[35] D. Cvetinović, A. Erić, N. Milutinović, P. Škobalj, and V. Bakić, "Thermodynamic Analysis of the Process of Decomposition of Hazardous Waste in Thermal Plasma with the use of Different Working Media," in *16th Conference on Sustainable Development of Energy, Water and Environment Systems*, 2021, p. 726.

[36] A. Erić, D. Cvetinović, N. Milutinović, P. Škobalj, and V. Bakić, "Combined parametric modelling of biomass devolatilisation process," *Renew Energy*, vol. 193, pp. 13–22, Jun. 2022, doi: 10.1016/j.renene.2022.04.129.

[37] P. Atkins and J. de Paula, *Physical chemistry*, no. 8. Oxford University Press, 2015. doi: 10.1016/0016-0032(61)90671-8.

[38] G. v. Belov, V. S. Iorish, and V. S. Yungman, "IVTANTHERMO for Windows - database on thermodynamic properties and related software," *CALPHAD*, vol. 23, no. 2, pp. 173–180, 1999, doi: 10.1016/S0364-5916(99)00023-1.